Journal of Chromatography, 467 (1989) 75–84
Elsevier Science Publishers B.V., Amsterdam — Printed in The Netherlands

CHROM. 21 228

SELECTIVE DETECTION OF VOLATILE IRON COMPOUNDS BY FLAME PHOTOMETRY[a]

XUN-YUN SUN and WALTER A. AUE*
Department of Chemistry, Dalhousie University, Halifax, NS B3H 4J3 (Canada)
(Received December 21st, 1988)

SUMMARY

Volatile iron compounds respond in the flame photometric detector with good sensitivity and selectivity. For instance, the minimum detectable amount of ferrocene (signal-to-noise ratio = 2) is $1.0 \cdot 10^{-10}$ g or $5.4 \cdot 10^{-14}$ mol/s. Its linear range spans four orders of magnitude, and it responds $1.1 \cdot 10^{3}$ times stronger on a weight basis, or $1.5 \cdot 10^{4}$ times stronger on a mol (Fe/C) basis, than dodecane. Ferrocene response, at optimized conditions of high hydrogen and low air flow-rates, is suggested to arise from the chemiluminescent emission of a few of the prominent atomic iron lines in the ultraviolet (the less sensitive response from the stoichiometric hydrogen–air flame is spectrally more complex). Hydrocarbon-type quenching is minimal, *e.g.* it takes about 4800 ppm methane in the detector atmosphere to reduce the ferrocene peak by 50%. Conditions optimal for iron strongly suppress sulphur response. Various volatile iron compounds, including the pentacarbonyl, behave similar to ferrocene.

INTRODUCTION

Ferrocene [bis(cyclopentadienyl)iron] and many of its derivatives are stable, volatile compounds. Their number is large: several volumes of *Gmelins Handbuch* are devoted exclusively to their description. They serve in a variety of roles, *e.g.* as additives to flames (antiknock compounds), as stabilizers of lubricants and polymers, as photosensitizers, etc. Some have also insecticidal properties[1]. Although many ferrocenes may merely represent the elegant answer to a non-existing problem, there does exist a need for the sensitive, selective, and individual determination of a few of them. The fact that iron is an element ubiquitous in internal and external human endeavors —besides being fairly toxic[2]— further supports the general interest in its analytical methodology.

Earlier uses of ferrocenes suggest that the method of their determination should be able to cope with matrices of a predominantly hydrocarbonaceous nature and, at the same time, allow for their speciation. As long as the ferrocenes (or other types of ferrous compounds such as carbonyls or chelates) are of the required volatility and

[a] This work is part of the doctoral thesis requirements of X.-Y. S.

0021-9673/89/$03.50

thermal stability, gas chromatography (GC) in conjunction with a selective detector appears to be the method of choice. Volatile iron compounds have been determined by GC almost from the beginning of this technique, by using non-selective detectors such as the thermal conductivity detector. This was mainly done to gauge the success of various organometallic syntheses. Ferrocene and iron pentacarbonyl, in particular, chromatograph easily and without evidence of premature decomposition. The relevant literature is well covered in several monographs[3–5].

A variety of techniques could undoubtedly be used for the sensitive and selective detection of ferrocenes after GC separation — methods such as GC–single-ion monitoring mass spectrometry (SIM-MS), GC–atomic absorption spectrometry (AAS), GC–ETV-AAS, GC–microwave-induced plasma emission spectrometry (MIP-ES), GC–direct-current plasma-ES, GC–inductively coupled plasma (ICP) atomic emission spectrometry, GC–ICP-MS, GC–atmospheric pressure ionization (API)-MS, etc. However, a conventional (*i.e.* a simple, rugged, and inexpensive) GC detector would seem preferable for most types of analysis.

One GC detector that does an excellent job on iron- (and some further metal) containing species is the hydrogen-rich flame ionization detector (HAFID)[6]. For ferrocene its minimum detectable amount is 2.1 pg, its linear range about three-and-a-half orders of magnitude, and its selectivity against hydrocarbons (tetradecane) approximately $1.9 \cdot 10^5$. Although the HAFID is, construction-wise, a relatively simple variant of the common flame ionization detector, the device is to our knowledge not available in commercial form.

Among the commercially available units, the flame photometric detector (FPD) was shown, quite some time ago, to respond to ferrocene. The minimum detectable limit was then about 2 ng and the linear range more than two orders of magnitude. However, this result was obtained in a survey of compounds containing a larger variety of hetero-elements. The detector conditions were uniform for all analytes, and the spectral features that gave rise to the various luminescences were not investigated. Besides, ferrocene was the only iron compound tested[7].

It seemed reasonable, therefore, to re-investigate and optimize the FPD's response to iron-containing organometallics —the more so because the ferrocene analogue bis(cyclopentadienyl)ruthenium could recently be determined in an amount as low as $2 \cdot 10^{-12}$ g, or just about 1 fmol/s, by a (slightly modified) FPD[8].

Also, the FPD has been used primarily for *main*-group elements in the past. Besides the two for which it was developed and for which it is best known, phosphorus and sulphur, it also responds in an analytically useful way to tin, germanium, arsenic, selenium, boron and tellurium[9,10]. Aside from the present entry ruthenium, the only *transition* element from which the FPD was known for some time to produce significant levels of luminescene, was chromium[11]. The FPD in its various forms and response modes has been reviewed in detail in a recently published book[9], and several monographs on the subject are available.

Given the dearth of information on the behaviour of volatile iron compounds in the FPD, this study was designed to optimize ferrocene response, map the spectrum of its luminescence, chromatograph additional iron compounds, establish calibration characteristics, and check for interference by hydrocarbons.

EXPERIMENTAL

All experimental work was carried out on a Shimadzu 4BMPF gas chromatograph carrying a dual-channel FPD. The 1 m × 3 mm I.D. borosilicate glass column was packed with 5% OV-101 on 45–60-mesh Chromosorb W, and used under a nitrogen flow-rate of 32 ml/min. The column temperature was usually chosen such that the respective analyte would elute at a retention time of about 2 min (*e.g.*, 130°C for ferrocene). The injection port and detector base temperatures were 200 and 170°C, respectively. A simple resistance (R)–capacitance (C) filter (R = 10 kΩ, C = 200 μF) was inserted between electrometer and stripchart recorder. Other operating conditions are noted in the text or in the legends. The FPD outlet was situated directly under an efficient exhaust duct.

For spectral purposes, one of the photomultiplier channels of the FPD was replaced by a Jarrel-Ash Model 82-415 quarter-meter monochromator with a 1180-groves/mm grating blazed for 500 nm, and 2.0- (or, when possible, 0.5-) mm slits. The photomultiplier was the same as used for directly observing the luminescence in the FPD, *i.e.* a Hamamatsu R-268 tube (bialkali, 300–650 nm, maximum response at 420 nm). Two means of introduction were used to obtain the spectra: ferrocene was either repeatedly injected in solution and the wavelength drive adjusted stepwise by hand (which obviates the recording of possible background emissions), or ferrocene was coated onto Chromosorb W, filled into an empty column, and heated to a temperature that would produce the desired, constant level of analyte in nitrogen for an automatically scannable spectrum.

For analytical purposes, and unless stated otherwise, the FPD was operated *without* the conventional quartz chimney, adjustable flame shield and interference filter. A hydrogen flow-rate of 370 ml/min and an air flow-rate of 60 ml/min plus 23 ml/min additional nitrogen were piped into the detector to form the flame. (These are the "optimized" conditions referred to later in the text.)

The input of methane —used here as a simple hydrocarbon quencher— was slowly varied by injecting pure methane into an exponential dilution flask. This flask was inserted into the hydrogen supply line (which then joins the column effluent line before entering the detector volume). The concentration of quencher or additive is calculated on a *total* (not just on a hydrogen or column) flow basis.

Thermocouple-temperature measurements were made with fine and coarse wire thermocouple units via a simple amplifier (Omega OMNI-AMP II-A). The fine-wire (0.2 mm diameter) iron–constantan thermocouple was used with and without a coat of phosphoric acid.

RESULTS AND DISCUSSION

Fig. 1 shows a graph with typical data from one of the optimization runs. Here, the amount of air, hence the temperature, is varied over a larger range. The response —*i.e.* the luminescence emitted upon introduction of ferrocene— increases steadily with the air flow. Note that "response" includes any spectral feature within the purview of the photomultiplier tube. We shall discuss this behaviour later in the context of possible excitation processes.

Unfortunately but not unexpectedly, the baseline noise also increases with in-

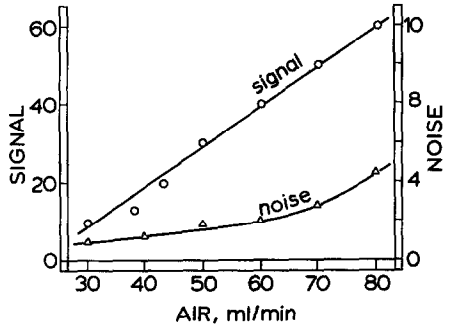

Fig. 1. Increase of signal and noise with increasing air supply. Analyte: ferrocene. Hydrogen flow-rate: 250 ml/min. No quartz chimney, no flame shield, and no optical discrimination. Other conditions as given in the experimental section.

creasing air flow-rate, *i.e.* with temperature and baseline current, and it does so in an apparently exponential fashion. This means that the signal-to-noise (S/N) ratios will reach maxima, and a few of these maxima are shown in Fig. 2. The highest S/N ratio is obtained at about 370 ml/min hydrogen and 60 ml/min air (plus 23 ml/min nitrogen added to the air supply, and 32 ml/min nitrogen coming from the column).

The optimum hydrogen flow-rate here is quite high for an FPD (*cf.* ref. 9), but the optimum air flow-rate supplies only about 7% of the oxygen that would be required for a stoichiometric flame. At these conditions, the maximum temperature measurable by the thermocouple is 570°C at the base of the flame (compare the theoretical maximum temperature of a hydrogen–air flame of 2115°C[12]. It makes little difference whether thinner or thicker wires are used, or whether the thermocouple is coated with phosphoric acid. Clearly, this result has nothing to do with *excitation* temperatures. Furthermore, such measurements are notoriously vague in *diffusion* flames. Yet, they do provide a valuable and dramatic indication of how low a level of thermal (as opposed to chemical) energy is actually available.

Other optimization strategies were pursued as well. As noted in the Experimental section, the quartz chimney and the adjustable steel flame shield were removed, with small but noticeably beneficial effects. No changes were apparent on varying the injection port and detector base temperatures between 160 and 200°C.

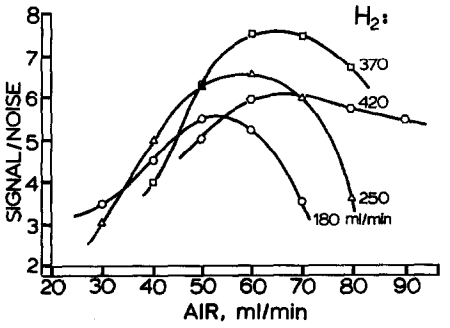

Fig. 2. Variation of the signal-to-noise ratio with varying air flow-rate, measured at four different hydrogen levels, as indicated. Other conditions as in Fig. 1.

(This suggests, *inter alia,* that no significant premature decomposition of ferrocene occurred in the chromatographic system.) Adding nitrogen to the air supply also improved performance, but larger amounts extinguished the flame.

Besides empirically optimizing the S/N ratio, analytical prudence suggests that the response spectrum be determined. This can serve to improve selectivity vis-à-vis other hetero-elements, and/or lead to better S/N ratios by the judicious use of optical filters. Also, it may on occasion yield results of general spectroscopic interest.

Fig. 3 shows a spectral scan of luminescence from a ferrocene-doped flame under conditions close to the analytical optimum. The peak width is determined by the very wide 2.0-mm slits (bandpath 6.7 nm), but that is all the low intensity and the diffuse nature of the luminescence would permit. The wavelengths of the peaks suggest that they represent some of the commonly found atomic lines. For instance, in a copper arc, the three strongest lines for transitions to the $^5D_4$ *ground* state are, in order of their intensity, 3719.94, 3859.91 and 3440.61 Å[13]. These numbers correspond, given our wide error limits, quite well to the peaks shown in Fig. 3 (373, 387 and 345 nm), although the latter might include more lines than the three cited ones. The strongest line in the copper arc is located at 3734.87 Å (from a 33 695 → 6928 cm^{-1} transition) and it may also be present here as well as become more prominent in the following spectra. Unfortunately, the inevitably low resolution does not allow us to distinguish among the several possible atomic emissions in the vicinity of 373 nm.

It seems reasonable to assume that the excitation process is chemical rather than thermal. The thermocouple temperature is fairly low (maximum 570°C for optimum flow-rates as given in the Experimental section), and other prominent lines of iron —*e.g.* the one at 3581.20 Å (34 844 → 6928 cm^{-1}), which is second-most intense in a copper arc— do not (yet) show up. The fact that the three that do result from transitions to the *ground* state, is expected: there must be an upper energy limit to the chemiluminescence. Note that 344 nm corresponds to 3.60 eV or 348 kJ/mol, and 34 844 cm^{-1} to 4.32 eV or 417 kJ/mol. A second argument in favour of a chemi-

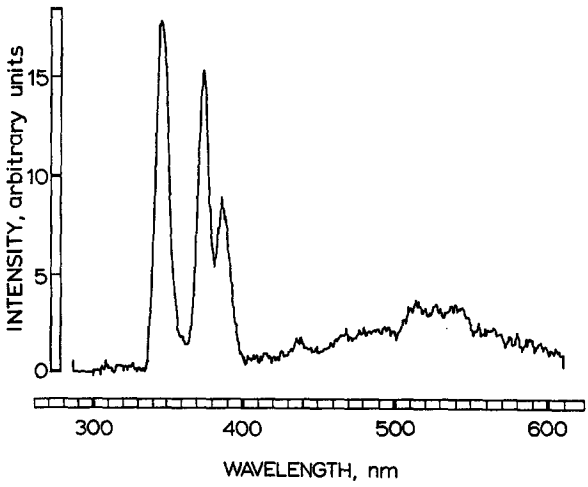

Fig. 3. Spectrum of "ferrocene", close to optimal flame conditions, but with a slightly higher air flow-rate (80 ml/min) to produce sufficient light. Slits: 2.0 mm (6.7 nm bandpath).

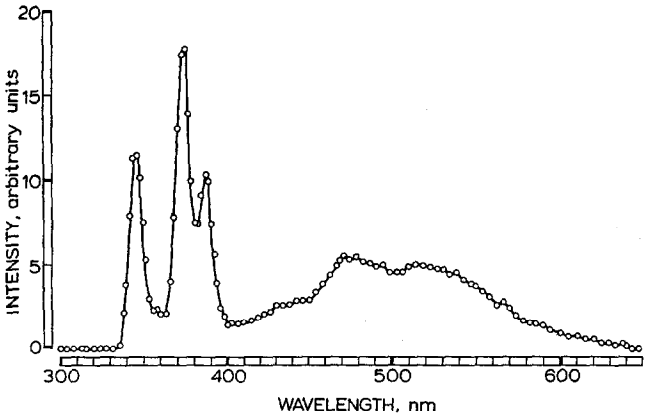

Fig. 4. Spectrum of "ferrocene", air-richer (81 ml/min) and hydrogen-poorer (260 ml/min) than at optimal conditions. Slits: 2.0 mm.

luminescent excitation process is an indirect but, in our opinion, rather strong one. If the excitation process were thermal, many other elements should respond with commensurate strength. The fact that most of the ones we tested did not, consequently suggests *non*-thermal excitation.

With slightly lower hydrogen and higher air supply rates, the spectrum changes (Fig. 4). The peak at *ca.* 373 nm has increased; this may, but need not, be due to the emergence of the above-mentioned 3734.87 Å line (whose excited state is at *ca.* 4.18 eV or 403 kJ/mol above the ground state). Also, a broad feature is starting to emerge between about 400 and 600 nm.

In the next spectrum, shown in Fig. 5, the hydrogen flow-rate has been dramatically decreased to the point that the flame is now approximately stoichiometric. The

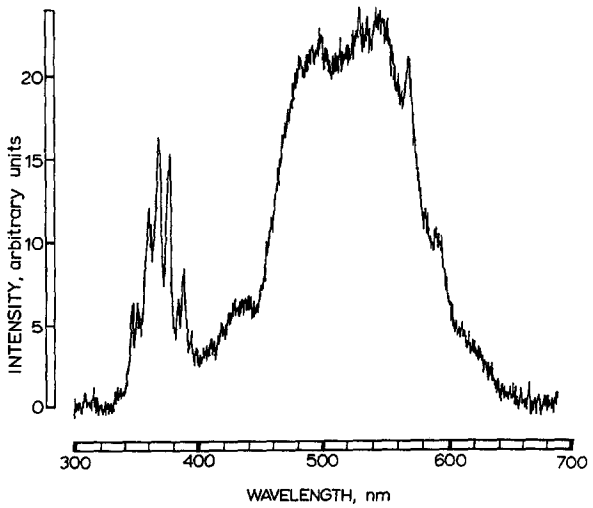

Fig. 5. Spectrum of "ferrocene", close to stoichiometric flame conditions. Hydrogen: 45.5 ml/min, air: 75 ml/min. Slits: 0.5 mm (bandpath 1.7 nm).

0.5-mm slits can be used because of the vastly increased light level. Some of the atomic lines may still be present, but they are now dwarfed by other features. In the ultraviolet, some new peaks have come up at *ca.* 359 and particularly at 367 nm; those may be related to the two groups of bands described by Gaydon as "probably FeOH. The first group lies in the region 3530–3580 Å and the second 3630–3675 Å, with a diffuse head, degraded to shorter wavelengths, at 3675 Å"[14]. Bands found in the hydrogen–air flame at *ca.* 344, 358, 383, 388 and 393 nm, and attributed[15] to FeO, may also be present; however, these may as well be due to prominent atomic lines originating from higher excited states of the iron atom[13]. The large hump between 460 and 580 nm must remain unassigned (perhaps it is even due to particle formation). The occurrence of FeH[16] and FeO[14] bands in that region cannot be ruled out; however, their contribution, if any, is not immediately apparent.

Note that Figs. 3 and 5 differ from Fig. 4 in that the former were run with a constant input of ferrocene and automatic wavelength scanning. Fig. 4, on the other hand, was determined by repeatedly injecting ferrocene while manually advancing the wavelength drive. Fig. 4 thus recorded the pure response, while emissions other than those resulting from ferrocene could have shown up in Figs. 3 and 5. However, scans of the blank flame in these cases confirmed that luminescence from the flame itself was negligible.

For analytical selectivity, the line at 344 nm or the lines at 372–374 (if they are indeed lines) would likely be the best bets for analysis with an interference filter. Another possibility may be to use a 400-nm cut-off filter, depending on what other FPD-active elements one wishes to guard against. However, the following calibration curves, with one exception as stated, have been established with no spectral discrimination whatsoever (beyond the response profile of the photomultiplier tube).

Fig. 6 shows several of such calibration curves for iron-containing analytes; plus, for purpose of comparison, one for a sulphur and two for a couple of hydrocarbon compounds.

The calibration curve for ferrocene under optimized conditions (curve 1) ends at a minimum detectable amount (S/N = 2) of 100 pg, or 10 pg/s, or 54 fmol/s. This is one order of magnitude better than found in the earlier survey[7]. The linear range spans four orders of magnitude. The selectivity against dodecane (which appears here as an alkane standard) is about $1.1 \cdot 10^3$, or $1.5 \cdot 10^4$ on an elemental (mol Fe/mol C) basis. In terms of a sensitivity ranking for the FPD, this performance places iron in the vicinity of sulphur and chromium (with only phosphorus, ruthenium, germanium and tin above it; and with arsenic, selenium, boron and tellurium clearly below it)[10].

Of course, this does not mean that sulphur would show up equally well at conditions optimized for *iron*. In particular, the absence of the quartz chimney decreases sulphur (but increases iron) response. Curve 7 shows the calibration for di-*tert.*-butyldisulphide, obtained under the same conditions as curve 1 for ferrocene. Not surprisingly, the selectivity of iron *versus* sulphur is now also much better than in the earlier study[7].

Curve 2 shows the calibration curve for ferrocene, but without the additional 23 ml/min nitrogen diluting the air supply (see the experimental section). The corresponding decrease in response is similar to that of ruthenocene[8].

Curve 3, which coincides with curve 2 over most of the graph, is that of iron pentacarbonyl. This compound is an interesting analyte in its own right, but it also

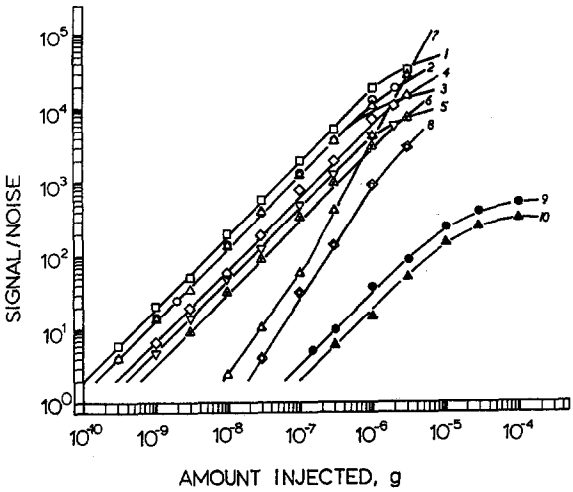

Fig. 6. Calibration curves: (1) Ferrocene at optimal conditions. Flow-rates in ml/min: hydrogen, 370; air, 60; carrier nitrogen, 32; additional nitrogen, 23. Temperatures in °C: column, 130; injection port, 200; detector base, 170. No quartz chimney. (2) Ferrocene. Conditions as in curve 1, but no additional nitrogen. (3) Iron pentacarbonyl. Conditions as in curve 1, but carrier nitrogen 11 and additional nitrogen 25 ml/min; column 35, injector 80 and detector 80°C. (4) Acetylferrocene. Conditions as in curve 1, but column temperature 180°C. (5) Ferrocene. Conditions as in curve 1, but original Shimadzu quartz chimney present. (6) Cyclooctatetraeneiron tricarbonyl. Conditions as in curve 1, but column temperature 150°C. (7) Di-*tert.*-butyldisulphide. Conditions as in curve 1, but column temperature 150°C. (8) Ferrocene. Conditions as in curve 1, but hydrogen 37 and air 83 ml/min (close to stoichiometric); 460 nm cut-on and 580 nm cut-off filter. (9) Naphthalene. Conditions as in curve 1, but column temperature 125°C. (10) Dodecane. Conditions as in curve 1, but column temperature 118°C.

demonstrates that the metallocene structure is not a necessary criterion for response. Two further iron compounds, acetylferrocene and cyclooctatetraeneiron tricarbonyl, are shown in curves 4 and 6, respectively.

Curve 5 shows the determination of ferrocene, with the original quartz tube of the Shimadzu FPD re-inserted. This is the same effect as discussed in the ruthenocene paper[8] and we still have no cogent explanation to offer for it. Analytically, of course, the removal of the conventional quartz cylinder turns out to be highly beneficial.

Curve 8 shows the calibration of ferrocene under stoichiometric flame conditions, with cut-on and cut-off filters around the big amorphous feature shown in the spectrum of Fig. 5. Note that response *per se* is higher, but that this response is analytically barren because of the concomitant high noise level.

Curves 9 and 10 are those of an aromatic and an aliphatic hydrocarbon, which have been included here to characterize the behaviour of a possible hydrocarbon sample matrix. As is well known, aromatics produce somewhat higher light levels.

In flame photometric analysis, particularly when the flame is weak and cool, quenching can seriously reduce response. The classical example of this type of interference is the diminution of S_2 luminescence by co-eluting hydrocarbons. To test for the relative importance of quenching, Fig. 7 shows the decrease in response of ferrocene and dodecane, as caused by increasing amounts of methane in the detector atmosphere. It may be worth noting that methane affects its homologue dodecane stronger than it does ferrocene.

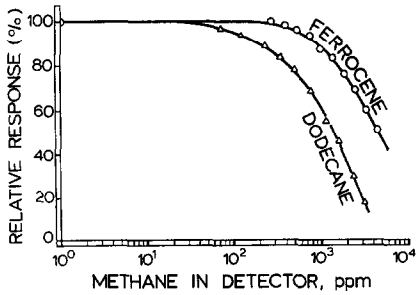

Fig. 7. Quenching of ferrocene and dodecane response by methane. Methane concentration given per total detector gas flow.

How serious is such quenching for the analyte ferrocene? It takes about $4.8 \cdot 10^3$ ppm methane in the total detector gases —corresponding to a carbon mass flow-rate of about 1 mg/min— to reduce the ferrocene peak by 50%. If methane had been doped only into the column flow, the corresponding concentration there would have been about 7%. That is far larger than any likely *continuous* input due to contamination. If, on the other hand, the same level of interfering carbon compound had eluted *as a peak* of the same retention time as ferrocene, quenching would have been observed only in the upper regions of the calibration curve. In its lower regions, the interferent would have *added* to the peak height, *i.e.* its own response would have been larger than the quenching it inflicted on the ferrocene response. The large amounts of carbon necessary to produce a 50% reduction in ferrocene peak height suggest that quenching should not present a serious problem under conventional circumstances.

Fig. 8 presents a temperature-programmed separation of six volatile iron compounds injected in 0.5–2-ng amounts. The chromatogram also shows 200 ng of a

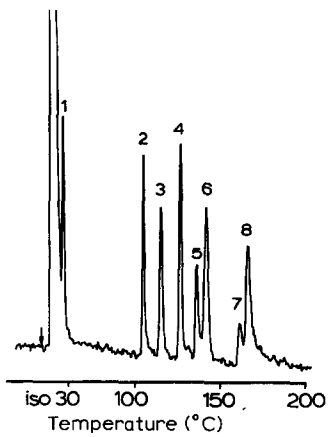

Fig. 8. Temperature-programmed chromatography at detector conditions optimal for ferrocene. Isothermal at 30°C until $Fe(CO)_5$ elutes, then 18°C/min till 100°C, then 10°C/min from 100 to 200°C. Peaks: 1 = 1 ng ironpentacarbonyl; 2 = 200 ng di-*tert.*-butyldisulphide; 3 = 800 ng dodecane; 4 = 1 ng ferrocene; 5 = 0.5 ng 1,1'-dimethylferrocene; 6 = 1 ng acetylferrocene; 7 = 0.5 ng ferrocene carboxaldehyde; 8 = 2 ng cyclooctatetraeneiron tricarbonyl.

disulphide and 800 ng of a hydrocarbon, which produce peaks of comparable size. This demonstrates graphically the point made earlier in regard to the corresponding calibration curves, *i.e.* that the normally large response of sulphur is diminished to a significant degree by choosing conditions optimal for iron compounds. Besides selectivity, the chromatogram also illustrates the sensitivity with which iron compounds respond. Given that the separation has taken place on a short, low-resolution packed column, still higher sensitivities could be expected from peaks of higher chromatographic efficiency.

ACKNOWLEDGEMENT

This study was supported by NSERC operating grant A-9604.

REFERENCES

1 *Gmelins Handbuch der Anorganischen Chemie, Vol. 14A, Ferrocen 1,* Springer, Berlin, 1974, p. 193.
2 N. Irving Sax, *Dangerous Properties of Industrial Materials,* Van Nostrand-Reinhold, New York, 5th ed, 1979.
3 G. Guiochon and C. Pommier, *Gas Chromatography in Inorganics and Organometallics,* Ann Arbor Sci. Publ., Ann Arbor, MI, 1973, p. 192.
4 P. C. Uden, in J. C. MacDonald (Editor), *Inorganic Chromatographic Analysis (Chemical Analysis,* Vol. 78), Wiley, New York, 1985, p. 263.
5 T. R. Crompton, *Comprehensive Organometallic Analysis,* Plenum, New York, 1987.
6 H. H. Hill, Jr. and W. A. Aue, *J. Chromatogr.,* 122 (1976) 515.
7 W. A. Aue and C. R. Hastings, *J. Chromatogr.,* 87 (1973) 232.
8 X.-Y. Sun and W. A. Aue, *Can. J. Chem.,* in press.
9 M. Dressler, *Selective Gas Chromatographic Detectors (Journal of Chromatography Library,* Vol. 36), Elsevier, Amsterdam, 1986, pp. 133–160.
10 C. G. Flinn and W. A. Aue, *Can. J. Spectrosc.,* 25 (1980) 141.
11 R. Ross and T. Shafik, *J. Chromatogr. Sci.,* 11 (1973) 46.
12 As cited in R. N. Kniseley, in J. A. Dean and T. C. Rains, (Editors) *Flame Emission and Atomic Absorption Spectrometry,* Vol. 1, Marcel Dekker, New York, 1969, p. 191.
13 W. F. Meggers, C. H. Corliss and B. F. Scribner, *Tables of Spectral-Line Intensities,* Part 1, NBS Monograph 145, National Bureau of Standards, U.S. Government Printing Office, Washington, DC, 2nd ed., 1975, p. 121.
14 R. W. B. Pearse and A. G. Gaydon, *The Identification of Molecular Spectra,* Chapman & Hall, London, 4th ed., 1976, p. 157
15 M. L. Parsons and P. M. McElfresh, *Flame Spectroscopy: Atlas of Spectral Lines,* IFI/Plenum, New York, 1971, p. 53.
16 P. K. Carroll and P. McCormack, *Astrophys. J.,* 177 (1972) L33.